

**STATISTICAL METHODS OF PHASE  
RECONSTRUCTION IN SPECKLE  
INTERFEROMETRY**

**A Thesis**

**Submitted for the Degree of**

**Doctor of Philosophy**

**in the Faculty of Science**

**by**

**SUBHASH KARBELKAR**



**DEPARTMENT OF PHYSICS  
INDIAN INSTITUTE OF SCIENCE  
BANGALORE-560 012**

**SEPTEMBER 1989**

## DECLARATION

I hereby declare that the work presented in this thesis is entirely original, and has been carried out by me at the Raman Research Institute under the auspices of the Department of Physics, Indian Institute of Science. I further declare that this has not formed the basis for the award of any degree, diploma, membership, associateship or similar title of any University or Institution.

**Sùbhash** Karbelkar

Department of Physics  
Indian Institute of Science  
Bangalore 560012  
INDIA

## ACKNOWLEDGEMENTS

The work presented here has been carried out at the **Raman** Research Institute under the auspices of Joint Astronomy Programme of the Physics Department, Indian Institute of Science. My thanks are due to both these Institutes for providing me such an excellent research opportunity. I wish to thank all the faculty of the Joint Astronomy Programme who did their best to initiate me in astronomy.

I thank Dr. N. Kumar and Dr. Chanda Jog for the interest they have maintained in my work in spite of **it being** far from the area of their own research.

I would like to thank all the members of the **Raman** Research Institute for providing an enjoyable and friendly atmosphere. Whomsoever I approached has been most willing to sort out the difficulties I encountered at different stages of my work.

The excellent library of the **Raman** Research Institute has provided invaluable support for my research work. It is a pleasure to thank Alina, Geetha, **Girija**, Ratnakar, Shobha and Vrinda for their help and cooperation.

I would like to thank Dipankar, Jayanthi, Johnson and Nata Raja for providing prompt computational help whenever I needed **it**.

My sincere thanks are due to Laksmi and Moksha for quick and accurate typing of manuscripts written over the years.

I would like to thank all my friends and colleagues at the Indian Institute of Science and at the **Raman** Research Institute who have made life enjoyable during my stay in Bangalore. A

special word of thanks to Sridhar for casting clouds (ITC ಒಕ್ಕಡೆ) over occasional gray moments and boosting up my spirit (which comes close to the Irish cream). To him I owe the alternative title of this thesis: Spekulations.

It would be undermining the affection of Dipankar and his family and Usha and her family to express a formal vote of thanks. These folks successfully simulated "sweet home" conditions far away from my own native place. Similarly, Kusum and her family at Nagpur and my sister's family have taken all my responsibilities on their shoulders: but for them I would not have had enjoyed the blissful life of a reseach scholar.

I am most grateful to my parents who have always been a source of inspiration. Without their understanding and unfailing encouragement this work would never have been possible.

And now the **doktorvater** **Rajaram** Nityananda. I would consider myself lucky for beeing associated with him during these maiden years of my research. It gave me an opportunity to learn the powers and limitations of an academician par excellence. For both these I am grateful to him.

I am grateful to the Publisher, Indian Academy of Sciences for his kind permission to include the Fig 0.3 which is taken from the **Proc.Ind.Aca.Sc. A18 (1943)**.

I thank **Rajaram**, Sridhar and Uday for many suggestions which I believe have lead to significant improvement of the presentation in the thesis. I also thank Hanumappa for his help and care in making copies of the thesis.

ERRATUM

Page Text line number What it is What it should be from top

E-1	1	ERRATUM	ERRATA
A-Z	16	being	being
D-1	14, 19, 26	dimensional	dimensional
a-Z	7	Detector quantum ...	q detector quantum ...
1	5	observe	observes
1Z	1Z	in a	in
13	17	inhomogeneities	inhomogeneities
13	ZZ	lense	lens
13	Z3	receproual	reciprocal
13	28	spekle	speckle
14	10	Astronomically	Astronomically
16	9	dominant	dominant
16	13	track	track of
16	Z3	build	built
17	1	binary binary	binary
17	Z0	conclusins	conclusions
17	Z0	belived	believed
2-3a	Fig. 2.3	function	function
2-10	Eq. 2.7	4) $k=b, j=0$	4) $k=b, j=b$
Z-11	Eq. 2.10	$p^2 = n^2 n^{z+b} - n^2 n^{z+b}$	$p^2 = n^2 n^{z+b} - n^2 n^{z+b}$
2-13	Eq. Z.1Z	$\lambda \langle \mu \rangle^2$	$\lambda \langle \mu \rangle^2$
Z-15	Eq. 2.18	14	28
Z-Z	Table Z.1	$\Delta m$ SNR $m$ SNR	$\Delta m$ SNR $\Delta m$ SNR
E-1	18	average n.	average n.
E-E	7	Appendix A	Appendix A3
4-6	13, 24	choise	choise
4-8	18	$(Y_1, Z_1)$	$(X_1, Y_1)$
4-11	18	empasizes	emphasizes
4-13	14, 24	weigh	weight
4-14	7	emphasis	emphasise
4-14	19	contribute	contributes
L-1T	10	oi wont	or wont
5-Z	6	choise	choise
S-ZZ	9	choise	choise
Z-3	Z	fainter	brighter
C-Z	9	it it	it

# *Statistical Methods of Phase Reconstruction in Speckle Interferometry (the book of speculations)*

## CONTENTS

<b>Dramatis Personae</b>	. . . . .	D-1
<b>0 Introduction</b>		
0.1	Ground based high resolution optical astronomy	1
0.2	Michelson approach to high resolution astronomy	6
0.3	Speckle interferometry .	10
0.4	Scope of the thesis . . . . .	12
0.5	Summary of the thesis .	15
<b>1 SNR for the bispectrum: scaling laws</b>		
1.1	Introduction . . . . .	1-1
1.2	SNR for bispectrum at high light levels .	1-4
1.3	SNR for bispectrum at low light levels .	1-7
<b>2 Detection of parity of a binary star in triple correlation speckle interferometry</b>		
2.0	Introduction . . . . .	2-1
2.1	Model of the point spread function .	2-7
2.2	Parity statistics for a binary: expression .	2-9
2.3	SNR for parity detection at low light levels .	2-11
2.4	Parity detection in the presence of sky background	2-14
2.5	Effects of various intensity distributions for pixels	2-16
2.6	SNR for parity detection at general light levels	2-17
2.7	SNR for autocorrelation . . . . .	2-20
2.8	Conclusions . . . . .	2-22
A2	Appendix . . . . .	2-25

3	General results for Poisson noise on image intensity correlations	
3.1	Introduction	3-1
3.2	General results for Poisson noise on image correlations	3-3
3.3	Conclusion	3-8
A3	Appendix	3-9
4	Parity detection using double correlation	
4.0	Introduction	4-1
4.1	Parity detection using double correlation	4-2
4.2	The PSFDC	4-8
4.3	SNR for parity detection using feature B	4-11
4.4	SNR for parity detection using feature A	4-15
4.5	Numerical results and discussion	4-22
A4	Appendix	4-24
5	"Edge" effects in parity detection using triple correlation	
5.1	Motivation	5-1
5.2	The triple correlation for a binary	5-3
5.3	Parity detection due to the feature E	5-7
5.4	Parity detection due to correlation ridges	5-10
5.5	Parity detection due to the feature A	5-14
5.6	A discussion	5-15
A5	Appendix	5-18
B5	Appendix	5-24
C5	Appendix First order parity statistics :SNR	5-28
C	CONCLUSIONS	C-1
R	REFERENCES	R-1

## DRAMATIS PERSONAE

$N_s$	Average number of speckles in a short exposure image of a point source
$N$	Average total number of photons in an exposure for a point source
$\mathcal{N}$	Average photon count per speckle in an exposure for a point source $\mathcal{N}_0$ : for a zeroth magnitude star
$n$	number of photons in a pixel
$\lambda$	wavelength (optical region) $k = 2\pi/\lambda$
$r_0$	Fried's parameter characterising atmospheric seeing
$l$	Parameter analogous to the Fried's in the single scale model used in chapters 4 and 5
$X, Y, Z$	Focal plane coordinates, Two dimensional vector notation suppressed unless required otherwise
$i$	main line $\sqrt{-1}$
$l, m, n$	Subscripts or dummy indices; discrete analogues of focal plane coordinates $X, Y, Z$ etc in units of speckle size; two dimensional, whenever necessary explicit components $i_1, i_2$ etc used
$D$	Telescope diameter
$R$	Telescope radius
$SNR$	Signal-to-noise ratio
$I(x)$	Focal plane intensity
$u, v \dots$	Spatial frequencies
$b$	Binary separation, two dimensional but the focal plane axes aligned so that the binary is along the first axis
$B$	the same in units of speckle size
$\mu_i$	Classical intensity in a realization at $i$ 'th pixel due to star 1
$\psi_{i-b}$	the same due to star 2
$UE$	Unbiased estimator
$PSF$	Point spread function, the focal plane intensity due to a point source, the system transfer function



$R(x)$	the same as PSF used in the text
$q$	Detector quantum efficiency: <b>optics+quantum</b>
$M$	Number of frames of data used
$S(x)$	Source structure
$I_u, R_u, S_u$	Fourier representations of $I(x), R(x), S(x)$
$KT$	The Knox-Thompson method
$TC$	The triple correlation method
$\sigma$	Focal plane size of the seeing disk
$\rho$	Focal plane size of a speckle
$N_0$	normalization: $\pi R^2 N_0$ is the total photon count by a zeroth magnitude star through the entire aperture
	Poisson average
$\langle \rangle$	Average over atmospheric fluctuations
$\delta_{ij}$	Kroneckerdelta: $\delta_{ij} = 1$ if $i=j$ and $\delta_{ij} = 0$ otherwise
$\delta_{ijk}$ etc	$\delta_{ijk} = \delta_{ij} \delta_{jk}$ ; $\delta_{ijkl} = \delta_{ij} \delta_{jkl}$ and so on.
$\alpha_1, \alpha_2$	Relative strengths of the binary componets

## INTRODUCTION

### 0.1 Ground based high resolution optical astronomy

The nature of experiments in astronomy is passive owing to the superhuman proportions of astronomical objects. The universe conducts its experiments and the astronomer observe astronomical objects when and where they pose for him. To have a more complete record of an astronomical phenomenon it is necessary to be able to record as faint a signal as possible. In addition, it is important to be able to observe finer details in the structure of astronomical objects. But for the earths atmosphere both these requirements for stretching our known universe would have been fulfilled by large telescopes. Ideally, a large telescope has a large collecting area and better ability to resolve angular features in astronomical images. However, the turbulent atmosphere limits the resolution in long exposure images to about one second of arc at optical wavelengths which is the angular resolution of a 10 cm telescope. Temperature induced random density fluctuations convected by atmospheric turbulence offer random refractive-index inhomogeneities to incoming light waves. By the time starlight reaches the entrance pupil of telescope it shows random variations of both phase and amplitude (Fig 0.1). A zeroth order description of wave propagation in a random atmosphere is to project the column desity of air above the telescope onto the pupil. Although one had an optically polished mirror to begin with the result of such a projection is an equivalent aberrated mirror. Although this simple picture gives only phase modulation it is a

correct indicator of what the atmosphere does to focal plane images. The variations in amplitude are perceived by the eye as scintillations: the so called twinkling of the stars. Typically, the field decorrelation length is about 10 cm in the optical region. By this we mean the random difference of phase of the wavefront at two points separated by 10 cm is about  $\pi$ . An interesting naked-eye observation (Minnaert 1940) is to look at the twinkling of a star near the horizon with the eyes crossed so that one sees two images, one formed within each eye. They show independent scintillations of intensity. One can think of the corrugated pupil plane wavefront (like the one shown in Fig 0.1) as made up of a large number of plane waves with different angles of arrival. Each of these will produce a bright spot with nearly diffraction limited size. To get a decorrelation length of the order of 10 cm the RMS angle of arrival of different waves forming the pupil plane field should be about 1". As a consequence the instantaneous image of a point source has a spread of about 1" (corresponding to the 10 cm decorrelation length) and contains many bright spots, the so called speckles, with nearly diffraction limited size (Fig 0.2b). These atmospheric corrugations change with time on a scale of typically 10 ms, resulting in a time dependent speckle pattern. Though at any instant the finest features (individual speckles) in the image have (nearly) diffraction limited size, on long exposure one records only the "envelope" seeing disk which is typically 1" wide (Fig 0.2c).

Nevertheless, ground-based high resolution astronomy is possible with various novel techniques (see references to reviews at the end). Techniques like lunar occultation and intensity interferometry are not affected by the turbulent atmosphere. The Michelson stellar interferometer combines light from two (or more) mirrors smaller than the field decorrelation length. Though this does not avoid the problems offered by the atmosphere entirely, the effect of the atmosphere takes a simpler form and can be compensated for. Speckle interferometry uses statistical methods of image reconstruction from a large number of short exposure images formed by large telescopes. Though speckle interferometry is affected most by the atmosphere, its large light gathering capacity makes it a powerful high resolution technique for faint objects. The present thesis deals with some aspects of speckle interferometry, but we briefly first describe the salient features of the other methods.

Lunar occultations: Since the angular size of the moon is much larger than the angular resolution obtainable by this technique, the occulting edge of the moon can be considered essentially straight. A strictly circular moon would give a 10 mas Poisson spot but deviations of more than 10 m from circularity would eliminate that. The formation of the intensity pattern on the ground can be understood in two steps. In the first step the diffraction due to the lunar edge results in intensity variations just outside the earth's atmosphere. The scale of intensity variation of the knife-edge pattern at this plane is about 10 m which is the Fresnel zone size corresponding

to the earth-moon distance of about 400,000 Km and  $\lambda = 5000 \text{ \AA}$ . The further propagation encounters nearly 10 Km of earth's turbulent atmosphere. The corresponding Fresnel length is about 5 cm. In addition refractive effects also result in intensity variations. Taking 1" as a typical angular deviation in the angle of arrival of rays the scale on which refractive effects can affect the fields is readily estimated to be about  $1" \times 10 \text{ Km} = 5 \text{ cm}$ . Both these length scales are smaller than the scale of variation of the intensity atop the atmosphere. The atmosphere can thus introduce scintillations on a 10 cm lengthscale but does not significantly scramble the knife-edge pattern produced by the moon. By using telescopes of size larger than 10 cm (yet less than the 10 m Fresnel length) the effect of scintillation can be averaged to yield the true intensity distribution at the top of the atmosphere. **In spite** of the limited coverage in the sky the relative simplicity of the instrumentation is a major advantage of this technique.

Intensity interferometry: Pioneered by Hanbury-Brown and Twiss, intensity interferometry is based on the following fundamental principle. If the bandwidth of the incoming light is restricted to a frequency range  $\Delta\nu$  then for timescales shorter than  $\tau = 1/\Delta\nu$  the source can be treated as a coherent one with a stable amplitude and phase. The structure of fields at the surface of the source, though very complicated (thermal), can be regarded as frozen in. The intensity distribution due to so complex a source shows variations both temporally (timescale  $\tau$ ) and spatially. The order of

magnitude of the spatial scales can be estimated as follows. At the location  $z$  of the observer the cone of radiation from the source  $D$  subtains an angle  $\theta \sim D/z$ . For nearly monochromatic light this gives rise to the transverse coherence length  $l_{\perp} \sim \lambda/\theta$  on which the intensity changes normal to the rays. The longitudinal coherence length  $l_{\parallel}$  comes about because different waves in the bandwidth beat with each other resulting in intensity variations over the longitudinal length scale  $l_{\parallel} = \frac{\lambda^2}{\Delta\lambda}$ . Thus measurement of  $l_{\perp}$  gives the angular size of the source. Is this description of intensity correlations valid in the optical region? The answer to this general question was given by **Dirac** a long time before the conception of the intensity interferometry. While dealing with interference of light from quantum standpoint, he states that the same photon interferes only with itself. One can summarize the relevant results from quantum-electrodynamics as the following rules. First of all, we agree to deal with quasimonochromatic light and do not probe length-scales smaller than the wavelength of light. Next, calculate the intensity distribution classically. This calculation involves diffraction and interference. If a detector, during its response time, is to receive a certain amount of energy  $E$  on the basis of the classical theory then the number  $N$  of photons it will receive is a Poisson distribution with mean number of photons corresponding to the classical energy ( $\bar{n} = E/h\nu$ ). It should be emphasized that the distribution of photons detected by two detectors is independent Poisson with the instantaneous (classical) fluxes as the means. The classical intensities are

not constant in general and vary both spatially and temporally. The correlations in the number of detected photons in two detectors appear only because of correlations in the classical intensities at the two detectors.

The Narrabri intensity interferometer has two telescopes of diameter 6.7 m with baselines upto 60 m. Its detector response bandwidth 100MHz allows it to probe the intensity variations on lengthscales larger than 300 cm. Allowing for 10% tolerance the intensity interferometer can tolerate path differences smaller than 30 cm! The path differences introduced by the turbulent atmosphere are of the order of  $10^{-2}$  cm. For the same reason the mirrors need not be very accurately designed (compared to the traditional requirement of a fraction of a wavelength) thus greatly reducing the cost of the 6 m telescopes. The telescopes being very large the effect of atmospheric scintillations is negligible. The measurement of diameters of the 32 stars by the Narrabri group stands as a "skymark" in optical high resolution astronomy. Incidentally, The duration of exposures in speckle interferometry is about 10 ms some  $10^6$  times the intensity coherence time  $10^{-9}$  s,  $\Delta\lambda = 100 \text{ \AA}$ , Thus as far as optical speckle interferometry is concerned one can safely neglect the Brown-Twiss intensity correlation and use Poisson statistics governed by the instantaneous intensity.

0.2 Michelson approach to high resolution astronomy  
The credit of first measuring angular size of distant stars, thus opening the new horizon of high resolution astronomy, goes to

Michelson<sup>[11]</sup> and Pease<sup>[12]</sup> who succeeded in overcoming the limitations imposed by the seeing. Extending Fizeau's idea of putting a mask with two small holes on the pupil of a telescope they attached a 20 ft beam with small mirrors mounted on it on the Mt. Wilson telescope. The beam with mirrors increased the effective baseline available with the 8-ft diameter Mt. Wilson telescope thus gaining resolution higher than the Rayleigh limit of the telescope; the latter alone wouldn't have been able to resolve some of the stars even in the absence of atmospheric degradation. More importantly, the use of mirrors of size smaller than the field decorrelation length simplified the nature of atmospheric noise and it was possible for them to measure the diameters of 8 stars. First, consider such an interferometer in the absence of atmospheric degradation. The image of a point source, for a telescope with a masked pupil with two holes, consists of the well-known Young's two hole fringes. The fringes have width corresponding to the separation between the two holes and the overall fringe pattern has an extension that corresponds to the size of the individual small mirrors. For example, if the size of the small holes is 10 cm and the separation between them is 5 m then the focal plane image of a point source will be a spot of size 1" with fringes of size 20 mas in it. A second nearby point source will give a fringe which will superpose onto the first fringe as the two sources are incoherent. The result of such addition of fringe intensities is a fringe with the same periodicity (this is property of the hole separation and a result that addition of any number of sinusoidals with



the same periodicity is a sinusoid with the same period) with shifted location of the maxima when compared to the one star fringe. The location of the fringe maxima is crucial in knowing the parity of the binary source. Parity of a binary is defined as the side of the brighter component of the binary and is the subject of the major part of this thesis. The location of the fringe due to the binary is intermediate to the locations of hypothetical fringes due to the component point sources. If one knows the locations of the two stars accurately then from the location of the binary fringe relative to the two stars it is possible to know the side of the brighter component. The minima of the two source fringe system **do not** have zero intensity in general as contrasted to the single point-source fringe. This leads to loss in the fringe visibility. For sources whose angular diameter is equal to the fringe width the loss of fringe visibility will be near total.

Atmospheric degradation takes a simple form for Michelson interferometry. As the mirrors are smaller than the decorrelation length one can approximate the corrugations in the wavefront due to the atmosphere as random phase shifts and random tilts in the wavefront. These random phase shifts and tilts are different at the two mirrors forming the baseline. The difference in the phase shifts at the two mirrors has the effect of changing the overall direction of the source: this reflects in the drift in the fringes. This random drift in the fringes is of the order of 1". Difference in the

tilts on the two mirrors reduces the overlap of the 1" spots produced by the two mirrors. The fringes arise only in the overlapping region. Since the fringes drift by more (in fact a lot more) than their width the location of the fringe contains no information about the parity of the binary. However, the loss in the fringe visibility can be seen ( **atleast** Michelson and Pease were able to meet the requirement by detectors inherited from their PAPA and MAMA) as a function of the baseline. Extending the baseline more than 20 ft posed serious stability problems to the then available technology. The system must be mechanically stable to optical accuracies. Even if this were so the random phase difference introduced by the atmosphere at the extremities of the baseline make it very difficult for the bare human eye to observe a rapidly changing fringe pattern. Efforts to extend the baseline to 50 ft this way did not meet with success and the beamy version of the Michelson interferometry was abandoned. Modern technology has made it possible to overcome these problems. The modern versions have independently mounted small mirrors from which light is combined at a central optical table. Different parts of the interferometer are controlled to optical accuracy by laser interferometers. In addition, the randomness introduced by the atmosphere, in the form of relative path differences and wavefront tilts, is actively (technical term adoptively) compensated for. The interferometer includes sensors which detect the changes due to the atmosphere and correct for them.

### 0.3 Speckle interferometry

As mentioned before, an instantaneous focal plane image of a point source shows a random speckle pattern. A sufficiently nearby source will produce an identical image. If two sources are within the so called isoplanatic patch then their light passes through almost identical turbulence in the atmosphere. This isoplanatic patch is very roughly  $10''$  at optical frequencies. Though the point source response is quite random the instantaneous image of a binary, for example, will have identical (at least for bright sources when photon noise is unimportant) speckle patterns corresponding to the two stars.

That the speckles do contain information about the nature of the source was demonstrated in 1943 in a classic experiment by G N Ramchandran (1943). The speckles were due to scattering from lycopodium powder. Fig 0.3 clearly shows the nature of the source which was imaged by a lens covered with a glass plate with lycopodium powder on it. In the astronomical context Labeyrie (1970) proposed and demonstrated, with Gezari and Stachnik (1971), the use of what is now known as speckle interferometry. The idea is to obtain (perhaps) a large number of short exposure images and obtain the power spectrum from each one of these. The power spectrum due to one frame has noise which can be reduced by averaging many short exposure films. In particular if the source lies in a single isoplanatic patch and  $R(X)$  denotes the instantaneous focal plane point spread function (PSF) (intensity pattern due

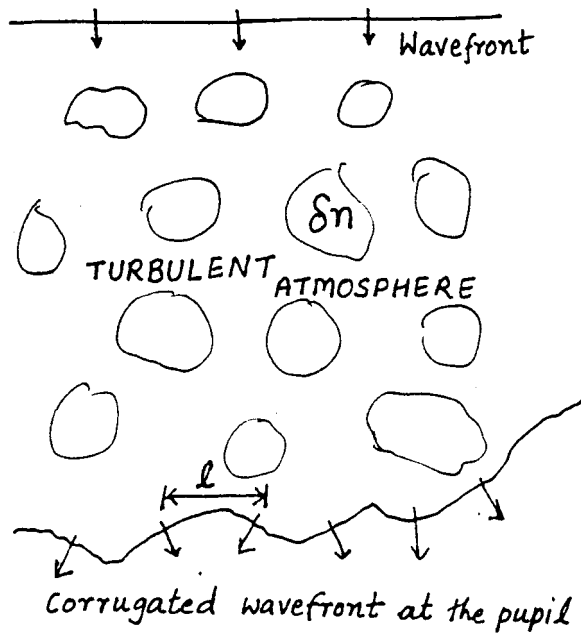


Fig 0.1 Wave propagation in random medium.

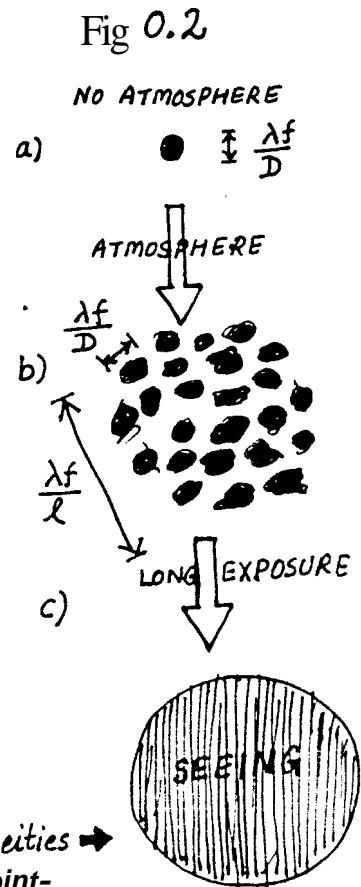
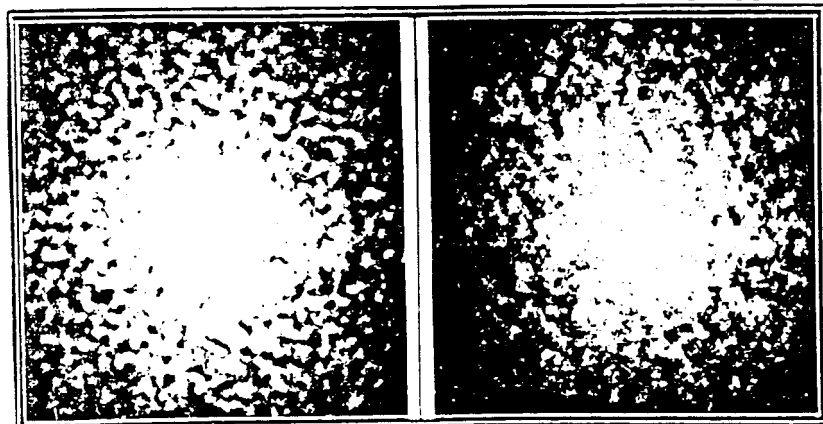


Fig 0.2 Effect of atmospheric inhomogeneities on the focal plane image of a point-source a) without and b) with atmosphere. c) the long exposure image.

Fig 0.3 Speckled image of a circular and triangular source



(Ramachandran G.N., Proc. Indian. Acad. Sc., A18, 1943)

to a point source located at the origin) and  $S(X)$  is the source structure then the instantaneous image is given by the convolution of  $R$  and  $S$ : which can be written in Fourier domain as

$$I_u = R_u S_u \quad I_u = \int d^2x e^{iux} I(x)$$

Speckle interferometry measures the power spectrum of the image and reconstructs the source power spectrum from this after correcting for the system response power spectrum which is measured for a nearby point source. As is obvious the power spectrum does not contain any information about the phases of the object distribution  $S_u$ . These phases are essential in unambiguous reconstruction of the object. The general second order correlation contains information about the object phases. However, because of properties of the system response there is a restriction on the Fourier components entering the general second order correlation:

$$\langle I_u I_{-u+\Delta u} \rangle \text{ nonzero if } |\Delta u| < \Delta u_{\text{max}} = r_0/\lambda f$$

This restriction comes because two widely separated Fourier components tend to be uncorrelated. Consider two nearby Fourier components. Each of these is a weighted sum of the focal plane intensity,  $I(X)$ . If  $\Delta u$  is smaller than the reciprocal of the seeing disk then the two weight functions will give almost the same integral. The existence of a second order statistic other than the power spectrum is an indicator that the focal plane image is not a stationary random process. If the seeing disk were of infinite extension when compared to the speckle size then power spectrum is the only second order statistics. The use of this general second order correlation was suggested by Knox and Thompson (1974). The **Knox-**

Thompson algorithm gives us the gradient (strictly the difference) of the source structure in the Fourier domain. The actual object phases are constructed recursively from the gradients. An alternative solution to the phase problem was proposed by Weigelt (1977) who proposed the use of the third order statistics, the so called bispectrum

$$\langle I_u I_v I_{-u-v} \rangle = \langle R_u R_{-u} R_{-u-v} \rangle S_u S_v S_{-u-v}$$

which contains the object closure phase from which object phases are recursively solved for. The only ambiguity in the restoration involves an overall shift in the object. Besides these techniques dealing with conventional (though short exposure) images from traditional telescopes there are other innovative schemes which combine the pupil plane fields in a different ways, for example the rotation shearing interferometer (Rodier [4] 1988). These are not discussed in this thesis.

#### 0.4 The scope of the thesis

This thesis deals with the Knox-Thompson and the triple correlation techniques of phase reconstruction. Particular emphasis is on the estimation of the signal to noise ratios of the techniques at both high and low light levels. The noise in measurements arises because of two main reasons. First of all atmospheric noise i.e. the fluctuations in the point spread function due to changing atmospheric conditions, needs to be considered. This is relevant for both the high and the low flux limits. The second source of noise is that due to the finite number of detected photons in a pixel. This is a quantum effect. Associated with these two sources of noise are the

parameters  $N_S$  and  $\mathcal{N}$ .  $N_S$  is the average number of speckles in a realization. For a telescope of a given diameter  $N_S$  quantifies the atmospheric noise. If  $\ell$  is the field decorrelation length then there are roughly  $\frac{D^2}{\ell^2}$  statistically independent areas in the pupil plane within which the field nearly uniform. The phases on two neighbouring coherence patches are statistically independent and have RMS phase difference about  $\pi$  i.e. path difference of  $\lambda/2$ . The wavefront tilt  $\lambda/(\frac{\ell}{2})$  is about 1". To represent these  $N_S$  phase values one would need  $N_S$  plane waves with appropriately chosen amplitudes and angles of arrival. This argument based on a single scale model for the pupil plane fields gives us the average number of speckles in a frame to be  $N_S \sim D^3/\ell^2$ . In reality, the multiscale turbulence gives a slightly different scaling. Refractive index inhomogeneities comparable to the telescope size or larger than it can steer the overall speckle pattern as their effect is well approximated by an overall tilt in the wavefront. In this thesis, for analytic simplicity, only single scale model for the pupil plane fields is considered. The new results reported here are argued to be generic and should be applicable to a multiscale model as well. Usually speckle is taken to mean a bright spot. However, because a lense filters out spatial frequencies higher than the reciprocal of the speckle size it is reasonable to imagine the focal plane made up of  $N_S$  independent speckle size areas. The speckle size is the correlation lengthscale for focal plane intensity. In chapter 2 we assume the statistics of the intensities on such independent areas to be a Rayleigh statistics. So in this technical sense a **speckle** need not be

abright spot (The Rayleigh statistics peaks at zero intensity). The intensities of the individual speckles can be considered as statistically independent as they correspond to the strengths of  $N_s$  independent plane waves forming the pupil plane field.

The total photon count  $N$  in an exposure comes from an area  $D^2$  so the area per speckle is  $\ell^4$ . Now if the average number of photons in a speckle is  $\mathcal{N}$  then the fluctuation in this is  $\mathcal{N}^{1/2}$  as the number of photons obeys the Poisson distribution for a fixed intensity. The noise is unimportant if  $\mathcal{N}^{1/2}$  is much larger than unity. Astronomically, for a 10 ms exposure, 1" seeing 100 Å bandwidth  $\mathcal{N}=1$  means 13. For brighter objects the image is nearly classical and the only noise is due to the atmospheric degradation. For this reason in the SNR expressions for brighter sources only  $N_s$  appears. We also note here that what is relevant is the detected number of photons so in all expressions the product  $q\mathcal{N}$  should appear and not the detector efficiency  $q$  or  $\mathcal{N}$  individually. So although we derive the formulae for  $q=1$  first in the final expressions appropriate powers of  $q$  are introduced. Since different frames of data are statistically independent the SNR for  $M$  frames of data is  $M^{1/2}$  times the SNR for one frame.

Throughout this thesis we talk of various orders of correlations. In the context of intensity correlations by order of a term we mean the power of  $\mathcal{N}$ . The physical motivation for this nomenclature is that for genuine high resolution techniques individual speckles are the basic statistical elements. One aim of the study reported here is to derive the scaling dependence of **SNRs** on these two parameters. These scalings should hold (**atleast**



approximately) in the more general and realistic multiscale case.

#### 0.5 Summary of the thesis

In chapter 1 we present SNR estimates for the bispectrum and the phase reconstruction based on it. The SNR estimates given are valid for both high and low flux levels. In this chapter we show that the power spectrum analysis has a better SNR than the SNR for the bispectrum analysis. This result was contrary to the then existing SNR calculations for the bispectrum. The same conclusion was also reached, independently by other groups.

The SNR for the focal plane triple correlation presented in chapter 2 are complementary to the frequency domain calculations reported in chapter 1. In chapter 2 we are interested in the SNR for the detection of the parity of a binary star. Parity is defined as the side of the brighter component and is discussed in detail in this thesis. Binary stars are perhaps the simplest sources for which some ambiguity ( $180^\circ$  in position angle) remains after measuring the power spectrum. Parity is also known to the binary star observers as quadrant ambiguity. Parity is important in some astronomical applications, examples being the recently observed 'companion' to SN 1987A and closely separated gravitational lens images. Quadrant ambiguity may play crucial role in determining the orbital parameters for a binary as in the case of 70 Tauri (McAlister 1988)<sup>[10]</sup>. Since one is dealing with a property of the source structure, rather than intermediate quantities like phase gradient or the bispectrum, one can meaningfully compare how different phase reconstruction methods fare in determining parity. **In addition** the simple nature of the

source facilitates explicit analytic calculations in the focal plane domain rather than the Fourier domain usually discussed. Parity is defined in this chapter as a special case of the focal plane triple correlation. The calculations are based on certain approximations of the point spread function. In chapter 5 these calculations are extended to take into account effects neglected in this chapter 2.

The Poisson fluctuations obeyed by the photons **introduces** bias terms dominant at low flux levels. It is necessary to obtain unbiased estimators for quantities of interest. In the third chapter we present results on the general (frequency or focal plane) Poisson results on the **N'th** order statistics. The diagrammatic technique for keeping track various terms and the generality of the results is believed to be new. Results of this chapter allow us to discuss issues related to the choice of weight function to determine the parity of the binary. Our main interest being the parity of a binary we have considered in chapters 4 and 5 the question of the optimum weight function for parity detection. Results derived in the third chapter have been used there.

In chapter 4 we consider second order methods like the Knox Thompson. The Knox-Thompson has traditionally been analysed in the Fourier transform domain. A given Fourier phase is build up by fitting a large number of phase difference measurements, a process which is difficult to analyse. A differnt approach, based on focal plane correlations is proposed. Our results show that the second order method of parity determination has a SNR that

depends linearly on the binary separation. This effect was entirely missed by previous calculations dealing with the SNR for the PSF rather than for the actual source. This dependence on the separation make the second order methods less reliable than the triple correlation methods when the binary separation is close to the resolution limit (except for unrealistically faint sources at greater than  $m$  18).

In chapter 5 we return to the SNR for parity detection using the triple correlation method. This calculation is the low flux extension of the results presented in the second chapter but takes into account various effects absent in the idealization of the PSF used in that chapter. Similar to the results of chapter 4 the SNR for the new "edge effects (due to the finite size of the seeing disk) considered in this chapter depends on the binary separation. However, for magnitudes relevant to the present day speckle interferometry and for binaries near the diffraction limit of the telescope we find that the SNR for parity detection is essentially that given by the simpler model of chapter 2.

Although this thesis deals with binaries, for which explicit calculations are possible, the conclusions arrived at are **belived** to be generic to complex sources with structure at the scale of the resolution limit of the telescope.